

Basic Study

Alleviation of acute pancreatitis-associated lung injury by inhibiting the p38 mitogen-activated protein kinase pathway in pulmonary microvascular endothelial cells

Xiao-Xin Zhang, Hao-Yang Wang, Xue-Fei Yang, Zi-Qi Lin, Na Shi, Chan-Juan Chen, Lin-Bo Yao, Xin-Min Yang, Jia Guo, Qing Xia, Ping Xue

ORCID number: Xiao-Xin Zhang 0000-0002-3196-6532; Hao-Yang Wang 0000-0003-2878-3548; Xue-Fei Yang 0000-0003-1514-3234; Zi-Qi Lin 0000-0002-0445-9607; Na Shi 0000-0001-6395-3122; Chan-Juan Chen 0000-0002-9853-2632; Lin-Bo Yao 0000-0001-9087-7030; Xin-Min Yang 0000-0002-9441-7119; Jia Guo 0000-0001-8221-5459; Qing Xia 0000-0003-4373-2722; Ping Xue 0000-0003-3935-4845.

Author contributions: Zhang XX, Guo J and Xue P obtained funding and designed the experiments; Zhang XX, Wang HY, Yang XF and Lin ZQ performed the experiments and literature search; Shi N, Chen CJ, Yao LB and Yang XM evaluated histological images and carried out a biochemical analysis; Zhang XX, Xia Q and Xue P wrote and revised the manuscript; All authors have read and approved the final manuscript.

Supported by National Natural Science Foundation of China, No. 81873107, No. 82004154 and No. 81573766; and Science and Technology Planning Program of Sichuan, No. 2019YFS0259.

Institutional animal care and use committee statement: The study

Xiao-Xin Zhang, Hao-Yang Wang, Xue-Fei Yang, Zi-Qi Lin, Na Shi, Chan-Juan Chen, Lin-Bo Yao, Xin-Min Yang, Jia Guo, Qing Xia, Ping Xue, Department of Integrated Traditional Chinese and Western Medicine, West China Hospital of Sichuan University, Chengdu 610041, Sichuan Province, China

Corresponding author: Ping Xue, MD, PhD, Professor, Department of Integrated Traditional Chinese and Western Medicine, West China Hospital of Sichuan University, No. 37 Guoxue Lane, Chengdu 610041, Sichuan Province, China. xueping@wchscu.cn

Abstract

BACKGROUND

Previous reports have suggested that the p38 mitogen-activated protein kinase signaling pathway is involved in the development of severe acute pancreatitis (SAP)-related acute lung injury (ALI). Inhibition of p38 by SB203580 blocked the inflammatory responses in SAP-ALI. However, the precise mechanism associated with p38 is unclear, particularly in pulmonary microvascular endothelial cell (PMVEC) injury.

AIM

To determine its role in the tumor necrosis factor- α (TNF- α)-induced inflammation and apoptosis of PMVECs *in vitro*. We then conducted *in vivo* experiments to confirm the effect of SB203580-mediated p38 inhibition on SAP-ALI.

METHODS

In vitro, PMVEC were transfected with mitogen-activated protein kinase kinase 6 (Glu), which constitutively activates p38, and then stimulated with TNF- α . Flow cytometry and western blotting were performed to detect the cell apoptosis and inflammatory cytokine levels, respectively. *In vivo*, SAP-ALI was induced by 5% sodium taurocholate and three different doses of SB203580 (2.5, 5.0 or 10.0 mg/kg) were intraperitoneally injected prior to SAP induction. SAP-ALI was assessed by performing pulmonary histopathology assays, measuring myeloperoxidase activity, conducting arterial blood gas analyses and measuring TNF- α , interleukin (IL)-1 β and IL-6 levels. Lung microvascular permeability was measured by determining bronchoalveolar lavage fluid protein concentration, Evans blue

was performed according to the Guidelines of Animal Care and Use Committee of West China Hospital of Sichuan University (protocol number, 2017082A).

Conflict-of-interest statement: The authors declare that they have no conflict of interest.

Data sharing statement: No additional data are available.

ARRIVE guidelines statement: The manuscript has been prepared and revised according to the ARRIVE guidelines.

Open-Access: This article is an open-access article that was selected by an in-house editor and fully peer-reviewed by external reviewers. It is distributed in accordance with the Creative Commons Attribution NonCommercial (CC BY-NC 4.0) license, which permits others to distribute, remix, adapt, build upon this work non-commercially, and license their derivative works on different terms, provided the original work is properly cited and the use is non-commercial. See: <http://creativecommons.org/licenses/by-nc/4.0/>

Manuscript source: Unsolicited manuscript

Specialty type: Gastroenterology and hepatology

Country/Territory of origin: China

Peer-review report's scientific quality classification

Grade A (Excellent): A
Grade B (Very good): 0
Grade C (Good): 0
Grade D (Fair): 0
Grade E (Poor): 0

Received: December 25, 2020

Peer-review started: December 26, 2020

First decision: January 29, 2021

Revised: February 6, 2021

Accepted: March 29, 2021

Article in press: March 29, 2021

Published online: May 14, 2021

P-Reviewer: Kozarek R

S-Editor: Zhang L

extravasation and ultrastructural changes in PMVECs. The apoptotic death of pulmonary cells was confirmed by performing a terminal deoxynucleotidyl transferase-mediated dUTP nick end labeling analysis and examining the Bcl2, Bax, Bim and cle-caspase3 levels. The proteins levels of P-p38, NFκB, IκB, P-signal transducer and activator of transcription-3, nuclear factor erythroid 2-related factor 2, HO-1 and Myd88 were detected in the lungs to further evaluate the potential mechanism underlying the protective effect of SB203580.

RESULTS

In vitro, mitogen-activated protein kinase (Glu) transfection resulted in higher apoptotic rates and cytokine (IL-1β and IL-6) levels in TNF-α-treated PMVECs. *In vivo*, SB203580 attenuated lung histopathological injury, decreased inflammatory activity (TNF-α, IL-1β, IL-6 and myeloperoxidase) and preserved pulmonary function. Furthermore, SB203580 significantly reversed changes in the bronchoalveolar lavage fluid protein concentration, Evans blue accumulation, terminal deoxynucleotidyl transferase-mediated dUTP nick end labeling-positive cell numbers, apoptosis-related proteins (cle-caspase3, Bim and Bax) and endothelial microstructure. Moreover, SB203580 significantly reduced the pulmonary P-p38, NFκB, P-signal transducer and activator of transcription-3 and Myd88 levels but increased the IκB and HO-1 levels.

CONCLUSION

p38 inhibition may protect against SAP-ALI by alleviating inflammation and the apoptotic death of PMVECs.

Key Words: Acute pancreatitis; Acute lung injury; Pulmonary microvascular endothelial cells; P38; SB203580; Apoptosis

©The Author(s) 2021. Published by Baishideng Publishing Group Inc. All rights reserved.

Core Tip: We explored the role of the p38 mitogen-activated protein kinase pathway in the tumor necrosis factor-alpha-induced inflammation and apoptosis of pulmonary microvascular endothelial cells *in vitro* and verified the effect of SB203580-mediated p38 inhibition on severe acute pancreatitis-related acute lung injury in rats. p38 mitogen-activated protein kinase overactivation promoted tumor necrosis factor-alpha-induced inflammatory cytokine expression and pulmonary microvascular endothelial cell apoptosis *in vitro*. SB203580 improved severe acute pancreatitis-related acute lung injury by downregulating P-p38, NFκB, P-SATA3 and Myd88 and upregulating IκB and HO-1, which alleviated inflammation and apoptotic cell death in rats.

Citation: Zhang XX, Wang HY, Yang XF, Lin ZQ, Shi N, Chen CJ, Yao LB, Yang XM, Guo J, Xia Q, Xue P. Alleviation of acute pancreatitis-associated lung injury by inhibiting the p38 mitogen-activated protein kinase pathway in pulmonary microvascular endothelial cells. *World J Gastroenterol* 2021; 27(18): 2141-2159

URL: <https://www.wjgnet.com/1007-9327/full/v27/i18/2141.htm>

DOI: <https://dx.doi.org/10.3748/wjg.v27.i18.2141>

INTRODUCTION

Acute pancreatitis (AP), a common gastrointestinal disease, ranges from a self-limiting disease to a severe condition with high mortality. The overall mortality rate is approximately 2%[1], while the mortality rate of severe AP (SAP) with distant organ dysfunction increases to 37%-50%[2]. To date, the pathogenesis of SAP has not been completely clarified, and no specific pharmacological therapies for SAP or its associated organ failure are available. The management of AP is mainly limited to supportive care. The lung is the most vulnerable organ in patients with SAP. Acute lung injury (ALI) or its more severe form, acute respiratory distress syndrome, is reported to occur in 10%-25% of patients with AP and accounts for up to 60% of AP-associated deaths[3,4]. Therefore, the identification of an effective therapy for AP-

L-Editor: Filipodia

P-Editor: Ma YJ



associated ALI is still urgently needed to decrease AP mortality.

ALI secondary to SAP is clinically and histologically indistinguishable from other indirect (sepsis, trauma or burns) or direct (*e.g.*, toxins or infection) insults to the lungs[5]. ALI is characterized by disruption of the alveolar capillary barrier, which increases endothelial and epithelial permeability, decreases lung compliance and impairs gas exchange[6]. Multiple biological processes are involved in the mechanisms of endothelial permeability, such as cytoskeletal rearrangements, assembly/disassembly of cell junctions and survival/death[7-9]. Pulmonary microvascular endothelial cells (PMVECs) line the interior of blood vessels and are an essential part of the blood and tissue microenvironment. They are major actors responding to insults related to ALI[10,11]. PMVECs are the main targets of humoral and cellular mediators during injury[12] and actively produce proinflammatory cytokines, increase the levels of adhesion molecules and secrete prothrombotic substances, promoting injury by transforming to a prothrombotic and proinflammatory phenotype to further activate the immune and hemostatic systems[4,8]. PMVECs are likely to be the first-line responders in efforts to prevent the development of SAP-associated ALI. Therefore, modulation of pulmonary vascular homeostasis is crucial for the successful treatment of AP-associated ALI.

p38 mitogen-activated protein kinase (p38 MAPK), a member of the serine/threonine kinase family, is ubiquitously expressed. It plays an important role in diverse processes including endocytosis, gene transcription, cell proliferation, cytokine production, apoptosis and cytoskeletal redistribution[8]. Therefore, unsurprisingly, p38 MAPK is involved in many cascades that result in the development of mild AP with limited pancreatic injury to SAP with ALI. In an experimental AP model, p38 MAPK activation was observed in the lungs as early as 2 h after model establishment[13], while p38 MAPK inhibitors (SB203580 or CNI-1493) alleviated pancreatic and pulmonary injury, limited cytokine increases and improved survival[14-16]. Currently, the precise mechanism by which the p38 MAPK signaling pathway regulates SAP-related ALI is unclear, particularly PMVEC injury. In this study, we overactivated p38 MAPK to define its role in the tumor necrosis factor- α (TNF- α)-induced inflammation and apoptosis of rat PMVECs *in vitro* and then investigated the effect of SB203580, a specific p38 MAPK inhibitor, on SAP rats with ALI *in vivo*.

MATERIALS AND METHODS

Cell culture

Rat PMVECs were obtained from the BeNa Culture Collection (338210, Beijing, China). Cells were identified according to staining with rat anti-factor VIII and binding of FITC-labeled lectin (Sigma, United States)[17]. The cells were cultured in DMEM (Thermo Fisher, United States) supplemented with 100 mL/L fetal bovine serum (BI, Australia), 50 U/mL penicillin and 50 μ g/mL streptomycin (Thermo Fisher, United States). PMVECs were maintained at 37 °C in a humidified atmosphere with 95 mL/L O₂ and 50 mL/L CO₂.

Mitogen-activated protein kinase kinase 6 (Glu) recombinant adenovirus construction and transduction

The MAPK pathway is comprised of three sequential dual-specificity kinases, and MAPK kinase (MKK) 6 is highly selective for p38 activation. Overexpression of activated MKK 6 (Glu) constitutively activates p38 MAPK[18,19]. Lentiviruses carrying either no inserted sequence (null) or the *MKK 6 (Glu)* gene were constructed by Wuhan PeptBio company limited China. PMVECs were infected with the lentivirus at a multiplicity of infection of 10 in the presence of 5 μ g/mL polybrene (Sigma, United States). After lentivirus infection, MKK 6 (Glu)-overexpressing cells and control cells were obtained *via* puromycin (2 μ g/mL) screening and analyzed using western blotting. When the cells reached 70%–80% confluence, they were treated with TNF- α (20 ng/mL) for the indicated times and then used for the subsequent analyses.

Flow cytometry

PMVEC apoptosis was assessed using an Annexin V-FITC/PI kit (4A Biotech, China). Briefly, PMVECs were detached using trypsin, washed with cold PBS, pelleted and resuspended in binding buffer. Then, 10 μ L of Annexin V was added, and they were incubated for 5 min in the dark. After mixing with 5 μ L of propidium iodide, the cells were analyzed using a flow cytometer (BD Biosciences, United States).

Animals

Adult male Sprague-Dawley rats ($n = 25$, 210-230 g) were purchased from the Experimental Animal Center of Sichuan University (Chengdu, China). The animals were housed at 22-25 °C on a 12 h day-night cycle and fed standard rodent chow and tap water *ad libitum* for 1 wk of acclimation. The animal experiments performed in this study were conducted in accordance with the National Institutes of Health Guide for the Care and Use of Laboratory Animals. The protocol was designed to minimize pain or discomfort to the animals and approved by the Animal Ethics Committee of West China Hospital of Sichuan University.

Induction of the SAP model and experimental groups

After fasting for 12 h, the SAP model was established by biliary-pancreatic duct injection of 50 g/L sodium taurocholate (Sigma, United States, 1 mL/kg) using a micropump at a speed of 0.2 mL/min[20]. In the sham group, the rats received the same volume of saline instead of sodium taurocholate. All rats received a saline injection subcutaneously to compensate for fluid loss during the surgery (20 mL/kg body weight). The rats were randomly divided into the SO group, SAP group and SAP + SB203580 group. The SAP + SB203580 group was further divided into low-dose (SB2.5 group), middle-dose (SB5 group) and high-dose (SB10 group) subgroups according to the dose of SB203580 (2.5 mg/kg, 5.0 mg/kg and 10.0 mg/kg, respectively, $n = 5$). SB203580 (Selleck, United States) was intraperitoneally administered before model establishment. The rats were sacrificed 12 h after model induction, and samples were harvested rapidly for subsequent analysis.

Arterial blood gas analysis

At the end of the experiment, arterial blood samples were collected by cardiac puncture. A blood gas analysis was performed to detect the partial pressure of oxygen (PaO₂) and oxygen saturation (SaO₂, Cobas b 123 Analyzer, Roche, Switzerland).

Bronchoalveolar lavage fluid collection

After opening the chest, the right lung was ligated. Bronchoalveolar lavage fluid (BALF) was collected through slow and careful lavage of the left lung with 2 mL of 4 °C PBS. Then, the fluid was centrifuged at 500 g for 5 min. The supernatant was collected and stored at -80 °C until the analyses of the protein concentration and cytokine levels.

Histological examination and terminal deoxynucleotidyl transferase-mediated dUTP nick end labeling staining

The pancreas and lung were fixed with 40 g/L formaldehyde for 24 h. The tissues were then embedded in paraffin, and continuously sliced at a 5 mm thickness for staining with hematoxylin and eosin. The pancreatic and pulmonary histological assessment was performed and scored by two pathologists using a microscope at 200 × magnification[21,22]. For the assessment of the apoptosis of lung tissue, terminal deoxynucleotidyl transferase-mediated dUTP nick end labeling (TUNEL) staining was performed with a commercially available In Situ Cell Death Detection Kit (Roche, Mannheim, Germany) according to the manufacturer's instructions.

Measurements of cytokines and BALF protein concentrations

Concentrations of TNF- α , interleukin (IL)-1 β and IL-6 in the serum and BALF were evaluated using ELISA kits according to the manufacturer's instructions (R and D Systems, United States). The BALF protein concentration was determined using a BCA kit (Thermo, United States).

Lung microvascular permeability analysis

Evans blue extravasation was used to quantify the capillary permeability in the lungs. A 10 g/L Evans Blue solution (20 mg/kg, Sigma-Aldrich, United States) was injected into the tail vein 1 h before exsanguination. PBS was used to flush the remaining Evans blue from the pulmonary vascular system. After the complete removal of blood, the left lung was removed, weighed, homogenized in formamide and incubated at 37 °C for 24 h. Finally, the supernatant was quantified spectrophotometrically at 620 nm.

Myeloperoxidase activity

Pulmonary myeloperoxidase (MPO) activity was measured using the method described by Dawra *et al*[23]. Briefly, lung tissue was homogenized in phosphate

buffer (100 mmol/L, pH 7.4) at 4 °C and centrifuged to pellet the tissues. The samples were then resuspended in phosphate buffer (100 mmol/L, pH 5.4) containing protease inhibitors, 5 g/L hexadecyl trimethyl ammonium bromide and 10 mmol/L EDTA and subjected to three rapid freeze-thaw cycles. The suspension was sonicated and centrifuged to obtain the supernatant. Twenty microliters of the supernatant were incubated with 200 μ L of phosphate buffer (pH 5.4) containing 5 g/L hexadecyl trimethyl ammonium bromide and 2 mmol/L 3,3',5,5'-tetramethylbenzidine for 3 min at room temperature followed by the addition of 50 μ L H₂O₂. The difference in the absorbance of this assay solution between 0 min and 3 min was measured at 655 nm at 37 °C with a microplate reader (BMG LABTECH, Germany). MPO activity was calculated from a human MPO standard curve, normalized to the protein concentration and reported as mU/mg protein.

Western blotting

Lysates from PMVECs or lung tissues were extracted with RIPA lysis buffer (Abcam, United Kingdom) supplemented with protease inhibitors (Roche, Germany). The total protein concentration was quantified using a BCA kit (Thermo, United States). The same amounts of protein were separated on 10% or 12% SDS-PAGE gels and transferred to a polyvinylidene fluoride membrane. Membranes were blocked with 50 g/L nonfat milk for 2 h at room temperature and subsequently incubated with the following primary antibodies overnight at 4 °C: P-p38 (1:2000), NF κ B (1:1000), I κ B (1:1000), cleaved caspase-3 (cle-casp3, 1:1000), P-signal transducer and activator of transcription-3 (P-STAT3, 1:1000), myeloid differentiation factor 88 (Myd88, 1:1000), nuclear factor erythroid 2-related factor 2 (Nrf2, 1:1000), Bax (1:1000) and Bim (1:1000) from CST, United States; IL-1 β (1:1000), heme oxygenase-1 (HO-1, 1:1000) and Bcl2 (1:1000) from Abcam, United States; and TNF- α (1:1000), IL-6 (1:1000) and β -actin (1:1000) from Proteintech, China. After rinsing with Tris-buffered saline containing Tween 20 (10 min, \times 3), the membranes were incubated with a secondary goat anti-rabbit (1:5000, Proteintech, China) or a goat anti-mouse IgG-HRP antibody (1:10000, Proteintech, China) for 1-2 h at room temperature. Finally, after washing, the membranes were imaged using a chemiluminescence detection system (Bio-Rad, United States) and analyzed with Image Lab software.

Transmission electron microscopy

A 2 mm³ peripheral specimen was fixed with 25 mL/L glutaraldehyde for 2 h and then washed with 0.1 mol/L phosphate buffer (PH 7.4, 10 min \times 3). After fixing the samples with 10 mL/L osmium tetroxide for 2 h, the specimens were dehydrated through a graded series of ethanol solutions and acetone and embedded in Epon 812 (Sigma, United States). Ultrathin sections were cut with an ultramicrotome (Leica, Germany). Finally, the sections were stained with uranyl acetate and lead citrate and examined using a JEM-1230 transmission electron microscope (JEOL, Japan).

Statistical analysis

All statistical tests were performed using SPSS 20.0 (SPSS, United States) by a biomedical statistician. Data are presented as the mean \pm SE for continuous variables or frequencies and percentages for categorical variables. Data were analyzed using one-way analysis of variance or the Kruskal-Wallis test. A *P* value of < 0.05 was considered statistically significant.

RESULTS

Overactivation of p38 MAPK aggravates TNF- α -induced apoptosis and inflammatory cytokine expression in PMVECs

We overexpressed a constitutively activated MKK6 (Glu) in PMVECs, which was confirmed to over activate p38 MAPK (Figure 1A). Then, the cells were incubated in the absence or presence of TNF- α . Flow cytometry analysis showed TNF- α induced apoptosis in both null and MKK (Glu) cells. Compared with the null groups, the apoptotic rate was significantly higher in the MKK (Glu) group treated with TNF- α (Figure 1B and 1C). Meanwhile, the levels of inflammatory cytokines (IL-6 and IL-1 β) were also significantly upregulated in the MKK (Glu) cells (Figure 1D and 1E).

SB203580 attenuates pancreatic damage in SAP rats

Representative images of hematoxylin and eosin staining of the pancreas were shown

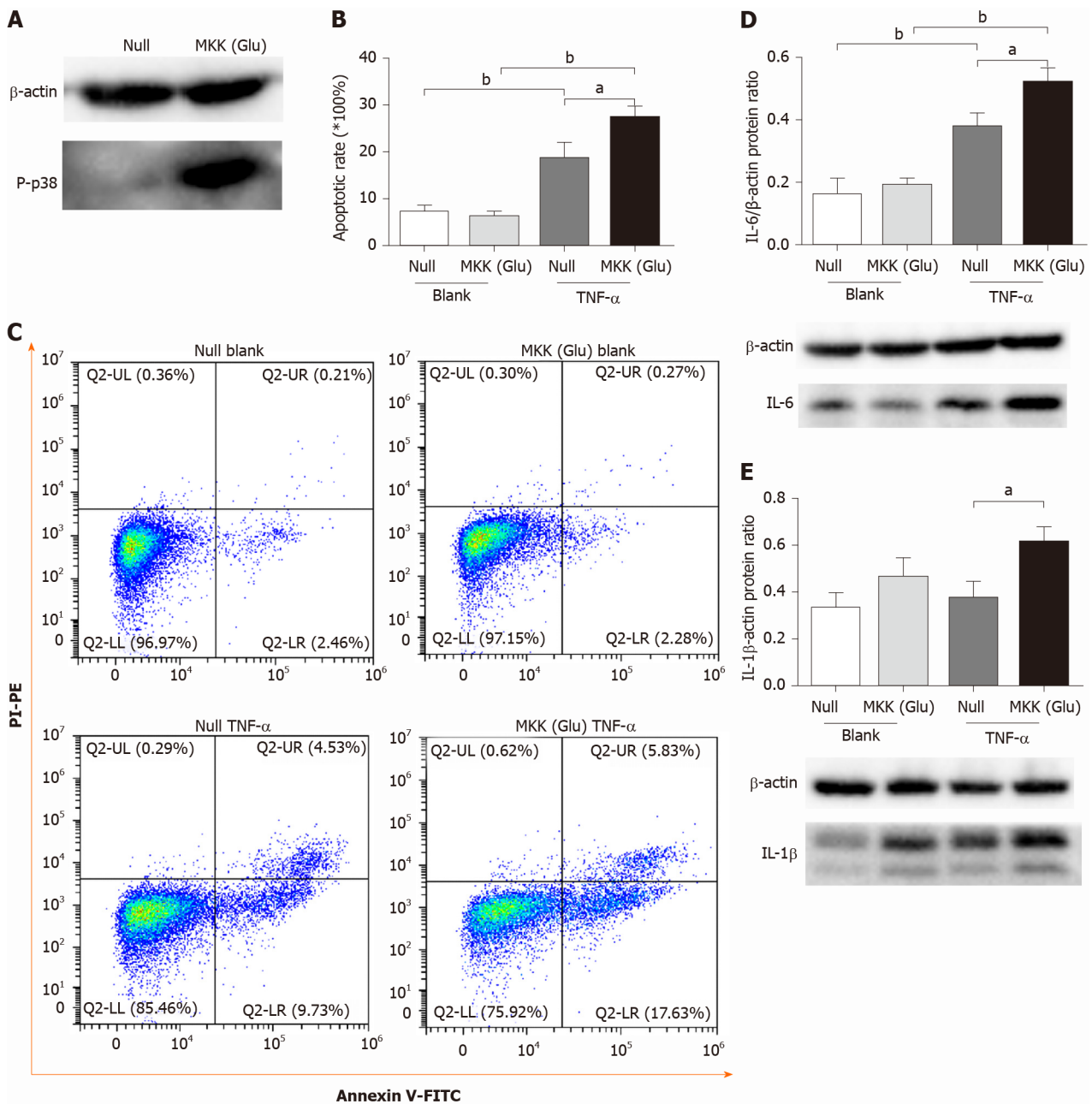


Figure 1 p38 mitogen-activated protein kinase overactivation aggravates tumor necrosis factor-alpha-induced apoptosis and inflammatory cytokine expression in pulmonary microvascular endothelial cells. A: Western blotting confirmed that mitogen-activated protein kinase (Glu) transfection constitutively activated p38 mitogen-activated protein kinase in pulmonary microvascular endothelial cells; B: Apoptotic rate in null and mitogen-activated protein kinase kinase (Glu) pulmonary microvascular endothelial cells stimulated with or without tumor necrosis factor-alpha for 24 h; C: Representative images of flow cytometry analysis for apoptosis; D: The expression level of interleukin-6 in each group; E: The expression level of interleukin-1β in each group. Data are expressed as mean ± SE of 3-4 samples per group; ^a*P* < 0.05; ^b*P* < 0.01. IL: Interleukin; MKK: Mitogen-activated protein kinase kinase; TNF-α: Tumor necrosis factor-alpha.

in Figure 2A. Except for slight pancreatic edema, no obvious changes indicative of AP were observed in sham-operated animals. Sodium taurocholate induced typical histopathological changes associated with AP, including diffuse edema, marked neutrophil infiltration, intrapancreatic hemorrhage and acinar cell necrosis. The histopathological scores were all significantly increased (Figure 2B-F). All three tested doses of SB203580 (2.5, 5.0 and 10.0 mg/kg) alleviated injury to the pancreatic tissues (all *P* < 0.05). We explored the difference in the therapeutic effect among the three different doses; compared to the SB2.5 group, 10.0 mg/kg SB203580 further significantly decreased the histopathological inflammatory infiltration, necrosis and total scores (Figure 2B, 2D and 2F).

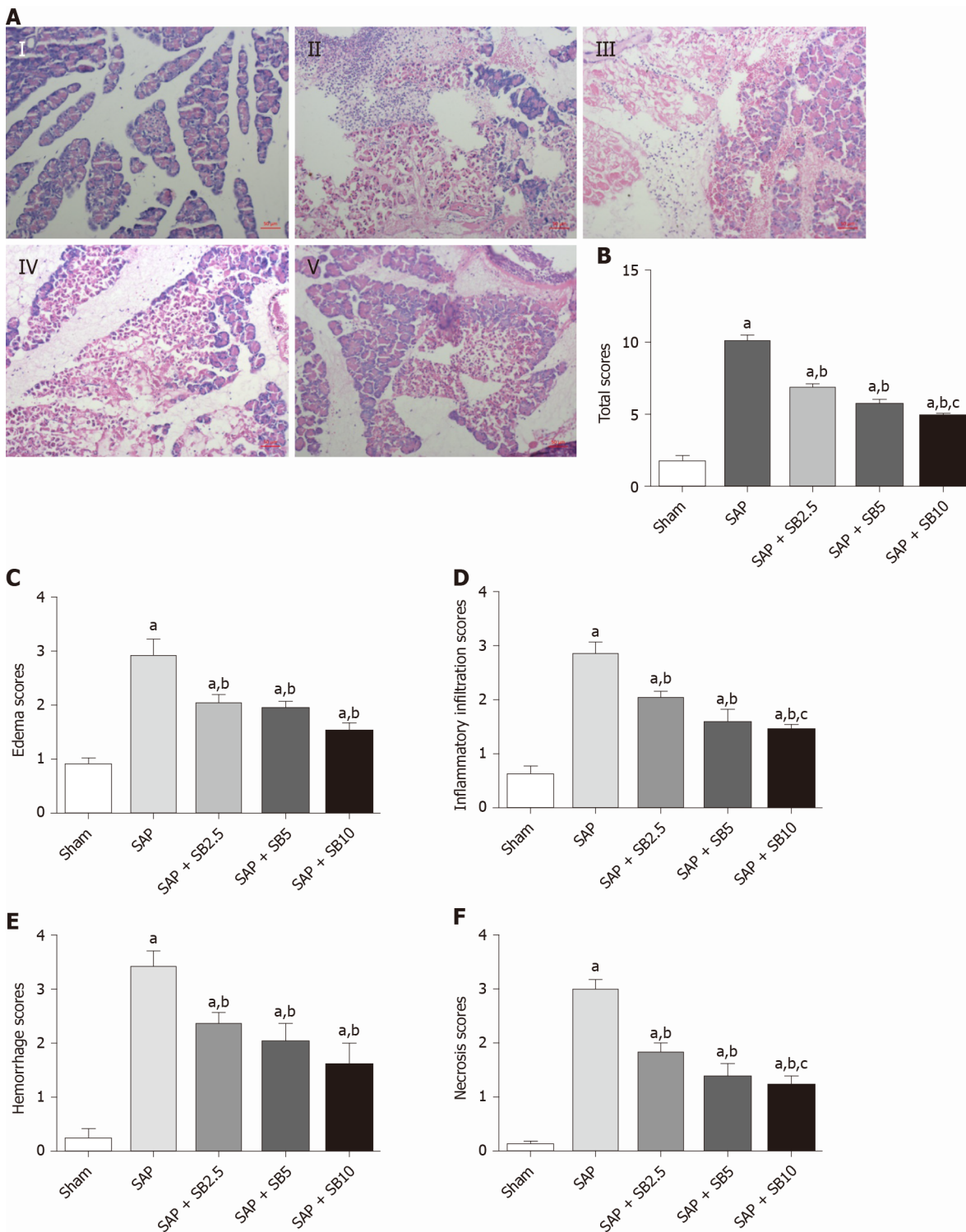


Figure 2 Effects of SB203580 on pancreatic histopathological changes and histopathological severity scores. A: Representative hematoxylin and eosin images of pancreatic sections (magnification 200 ×); I: Sham group; II: Severe acute pancreatitis (SAP) group; III: SAP + SB2.5 group; IV: SAP + SB5 group; V: SAP + SB10 group; B: Total scores; C: Edema scores; D: Inflammatory infiltration scores; E: Hemorrhage scores; F: Necrosis scores. B-F: Pancreatic histopathology scores in different groups; Data were expressed as mean ± SE; ^a*P* < 0.05 vs sham group; ^b*P* < 0.05 vs SAP group; ^c*P* < 0.05 vs SAP + SB2.5 group. SAP: Severe acute pancreatitis.

SB203580 alleviates lung injury in SAP rats

The histopathological changes in the pulmonary tissues were shown in **Figure 3A**. In SAP rats, lung damage was characterized by neutrophil infiltration, thickened alveolar walls, intra-alveolar hemorrhaging and alveolar collapse. The histopathological scores were also significantly increased (**Figure 3B-D**). These changes were accompanied by significantly increased IL-1 and TNF- α levels in the BALF and serum (**Figure 4A-D**)

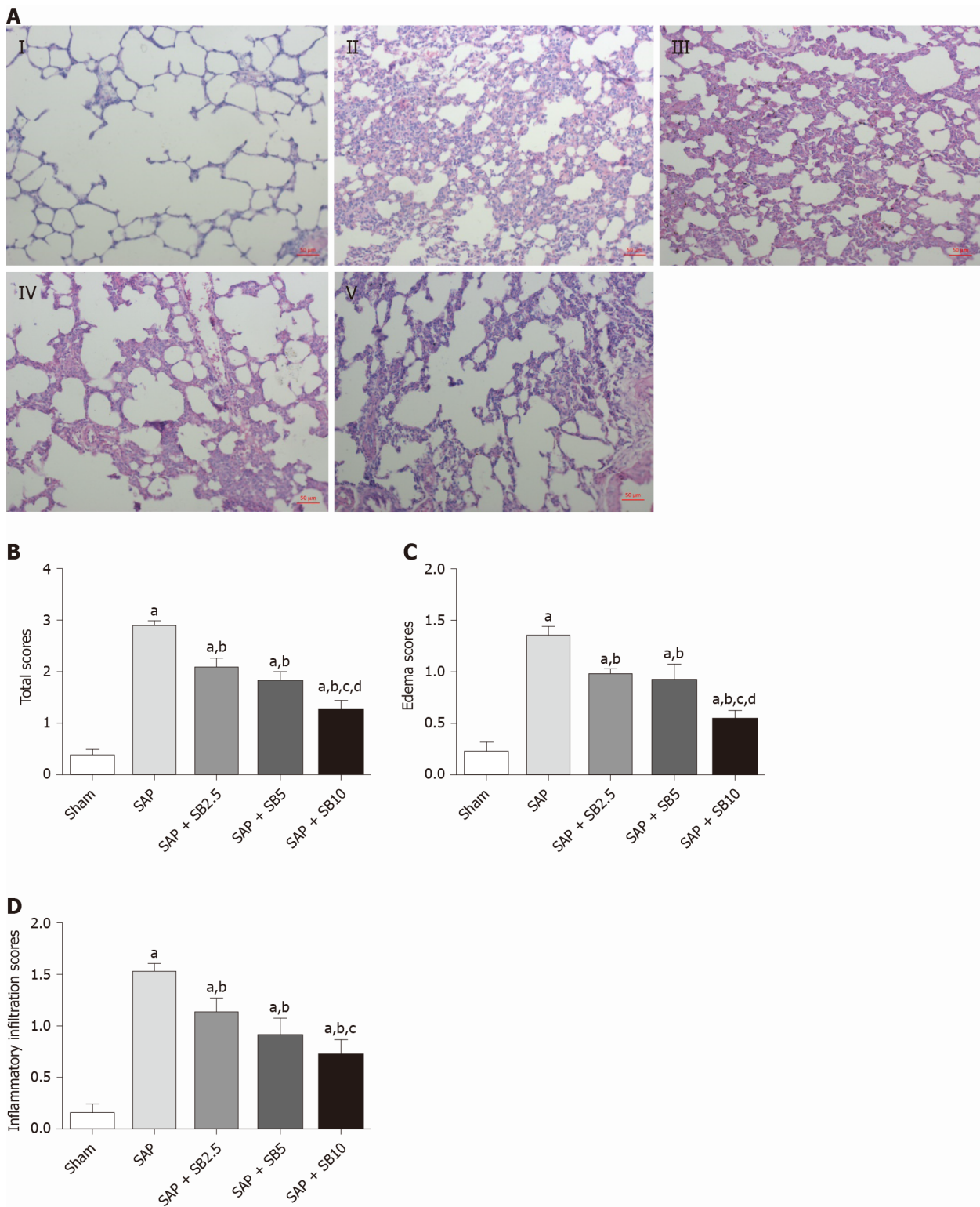
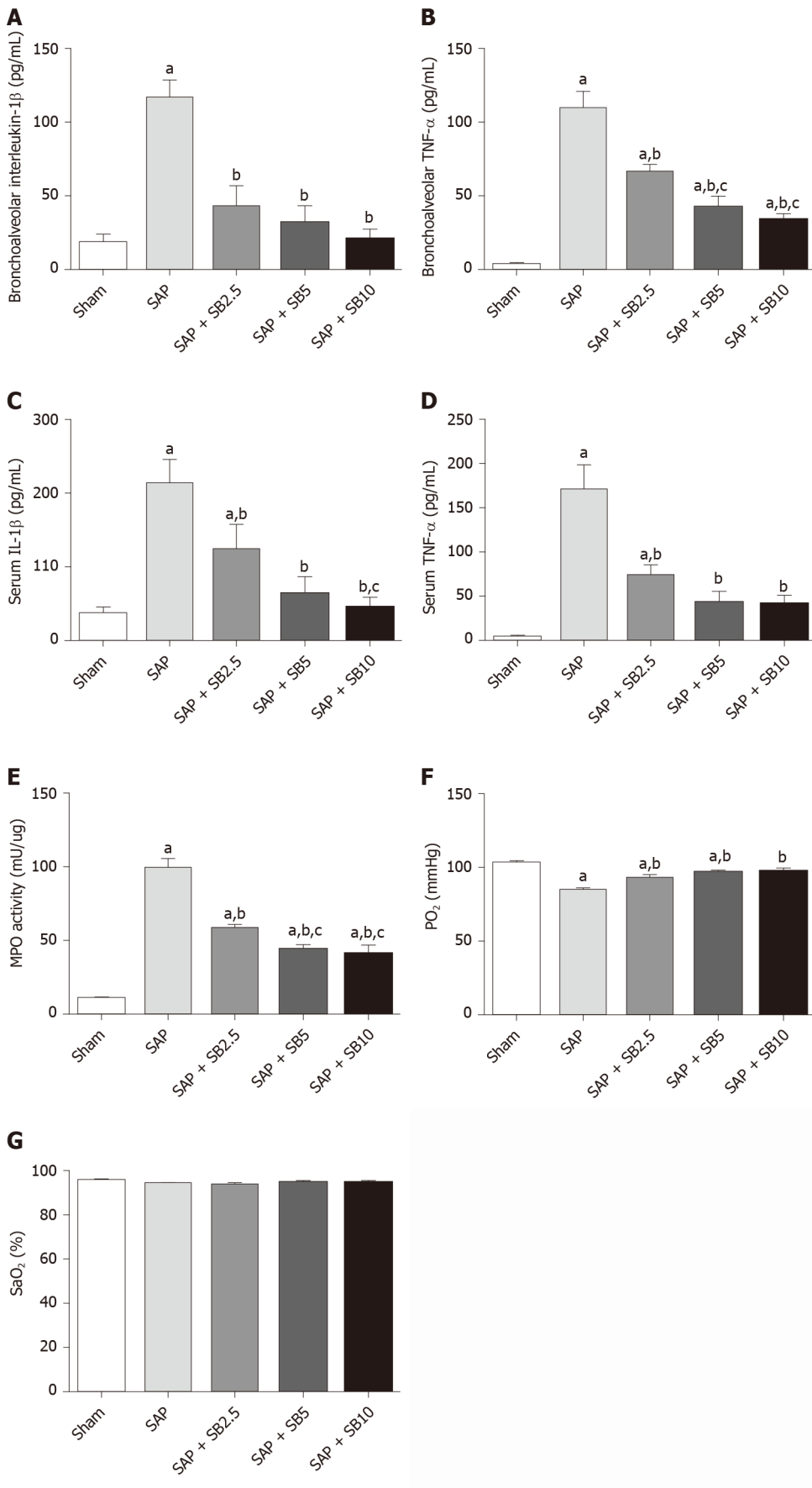


Figure 3 Effects of SB203580 on pulmonary histopathological changes and histopathological severity scores. A: Representative hematoxylin and eosin images of pulmonary sections (magnification 200 ×); I: Sham group; II: Severe acute pancreatitis (SAP) group; III: SAP + SB2.5 group; IV: SAP + SB5 group; V: SAP + SB10 group; B: Total scores. C: Edema scores; D: Inflammatory infiltration scores. B-D: Pulmonary histopathology scores in different groups; Data are expressed as mean ± SE of the mean; ^a*P* < 0.05 vs sham group; ^b*P* < 0.05 vs SAP group; ^c*P* < 0.05 vs SAP + SB2.5 group; ^d*P* < 0.05 vs SAP + SB5 group. SAP: Severe acute pancreatitis.

and pulmonary MPO activity (Figure 4E) and a decreased PaO₂ (Figure 4F). There was no change of SO₂ in the SAP rats (Figure 4G). At the same time, western blotting analysis also confirmed increased levels of inflammatory cytokines (IL-1, TNF-α, IL-6) in the SAP group compared with the sham group (Figure 4H-J). SB203580 treatment alleviated the histopathological injuries and scores, decreased the levels of inflam-



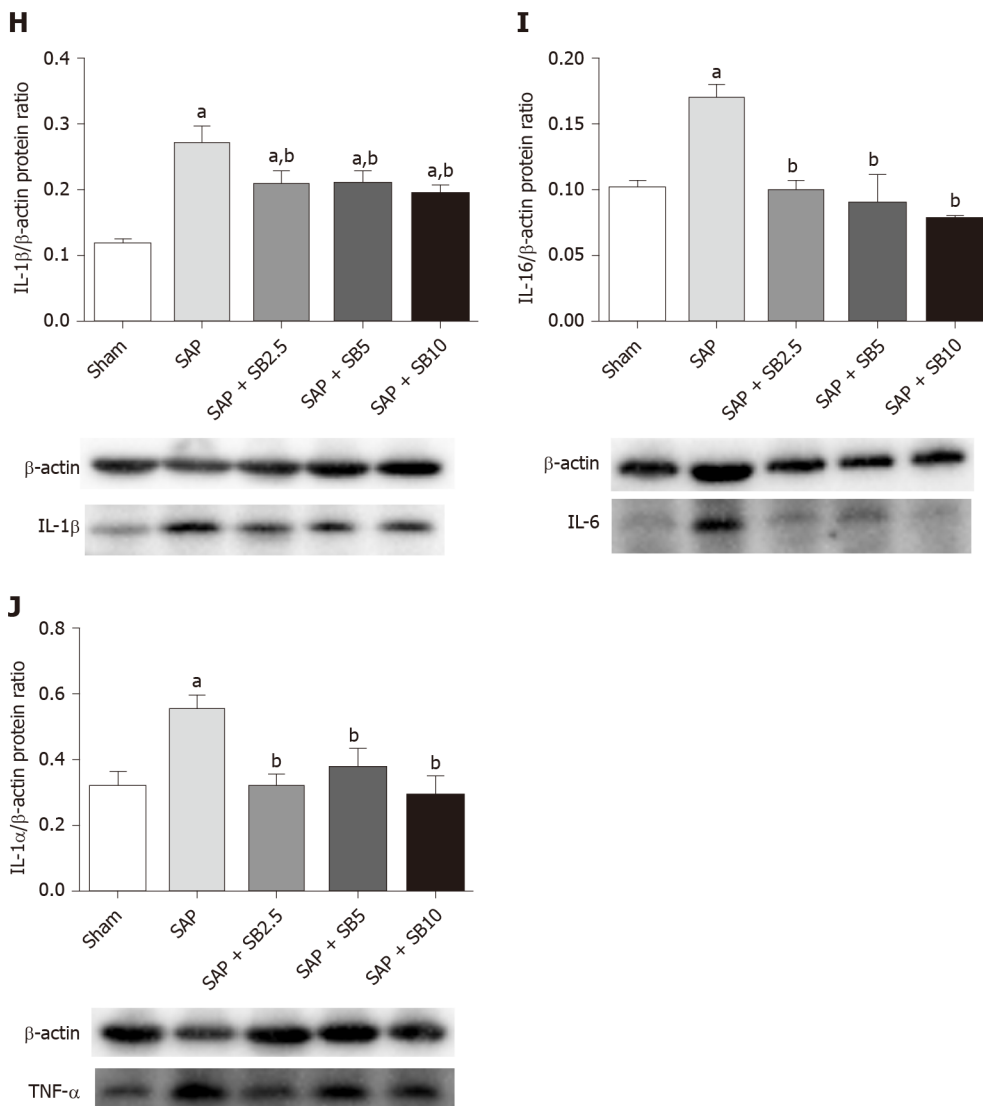


Figure 4 Effects of SB203580 on pulmonary severity indices of severe acute pancreatitis in rats. A: Bronchoalveolar interleukin-1β (IL-1β); B: Bronchoalveolar tumor necrosis factor alpha (TNF-α); C: Serum IL-1β; D: Serum TNF-α; E: Lung myeloperoxidase activity; F: Partial pressure of oxygen; G: Oxygen saturation; H: Representative western blotting analysis results for IL-1β in lung tissues; I: Representative western blotting analysis results for IL-6 in lung tissues; J: Representative western blotting analysis results for TNF-α in lung tissues. Data are expressed as mean ± SE of the mean; ^a*P* < 0.05 vs sham group; ^b*P* < 0.05 vs severe acute pancreatitis group; ^c*P* < 0.05 vs severe acute pancreatitis + SB2.5 group. IL: Interleukin; MPO: Myeloperoxidase; PaO₂: Pressure of oxygen; SaO₂: Oxygen saturation; SAP: Severe acute pancreatitis; TNF-α: Tumor necrosis factor-alpha.

matory factors (IL-1, TNF-α, IL-6 and MPO) and preserved PaO₂. Among the three doses tested, SB203580 at 10.0 mg/kg consistently and significantly reduced all histopathological and biochemical severity indices with the highest efficiency.

Protective effects of SB203580 on capillary injury

The permeability of the PMVECs was evaluated *in vivo* by measuring the BALF protein concentration and Evans blue accumulation in the lung tissue. Quantitative analysis showed a significant increase in these two parameters in SAP rats, which were suppressed by SB203580 cotreatment (Figure 5A and 5B). They further decreased after treatment with increasing SB203580 doses. The microstructure and integrity of the endothelium were evaluated using transmission electron microscopy. In the sham group, the lung tissues showed a normal capillary endothelium, as evidenced by an intact capillary basal membrane, dense endothelial cell-cell junctions and continuous and clear delineation between cells (Figure 5C). In the SAP group, capillary endothelial dissolution and rupture were noted. In addition, low electron density clouds with an irregular thickness indicating basal membrane edema, increased vacuolization, loose cellular junctions, swollen cellular organelles and nuclear degeneration were often observed. In contrast, the swelling and injury of endothelial cells were partially alleviated in lungs from SB203580-treated rats. After treatment with 10.0 mg/kg

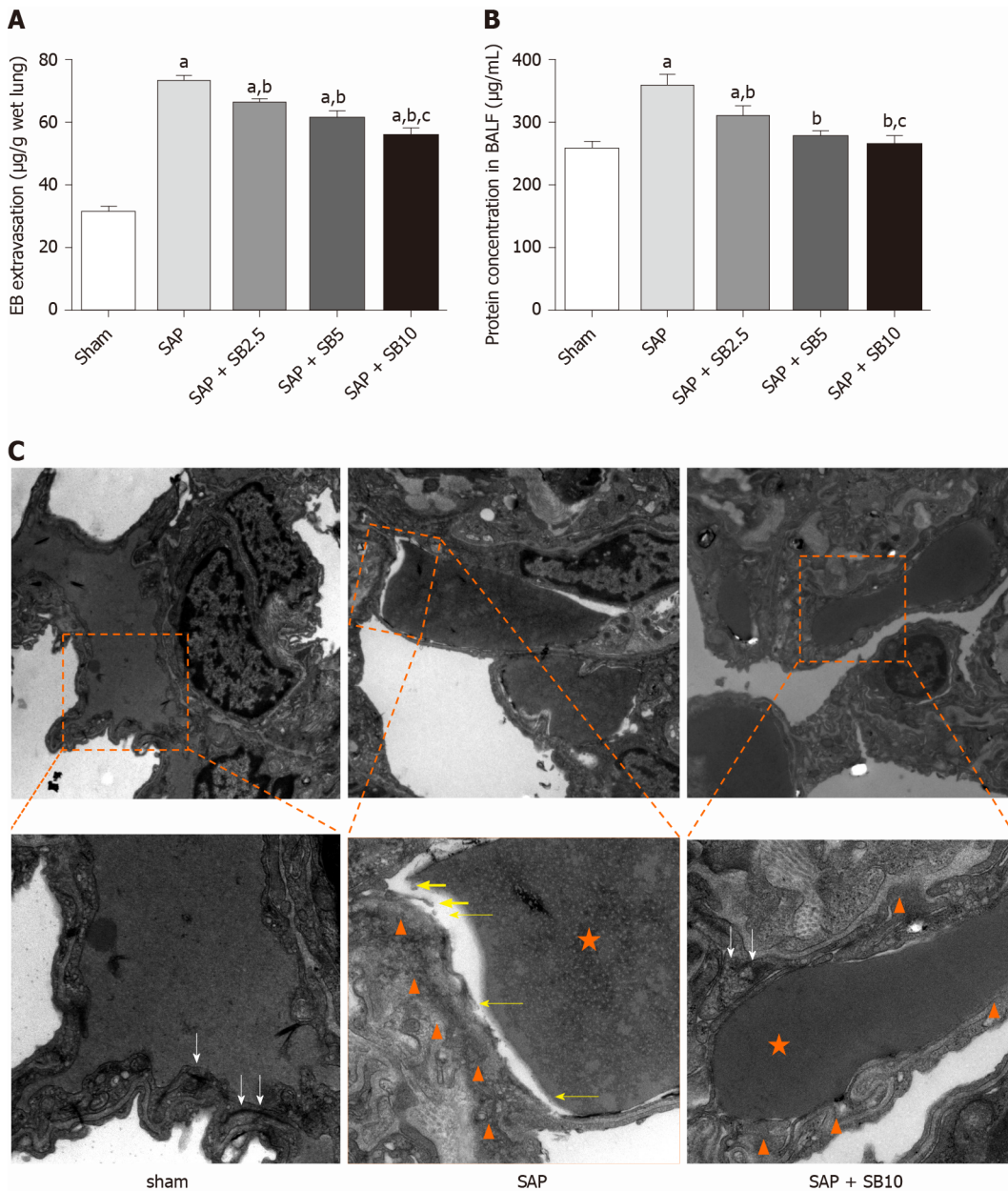
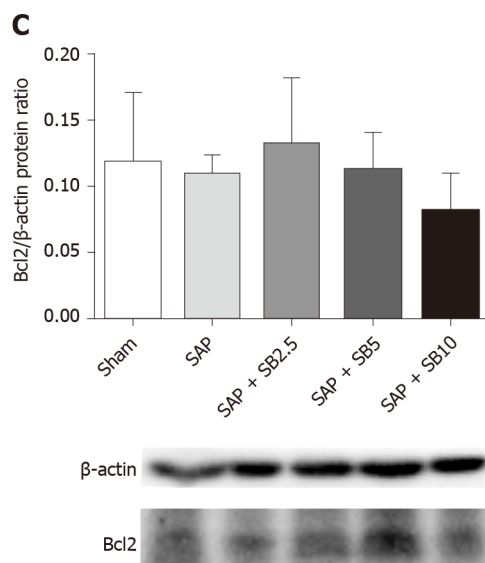
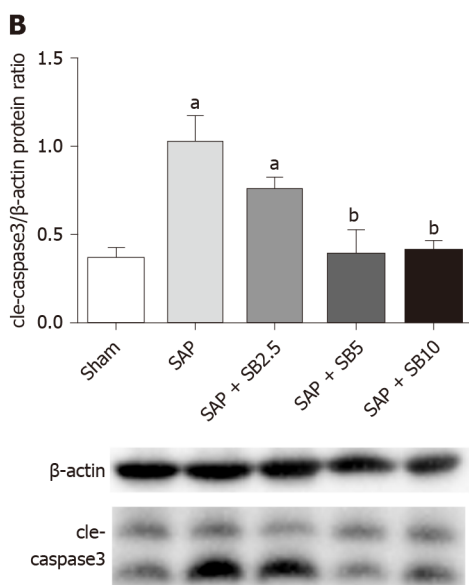
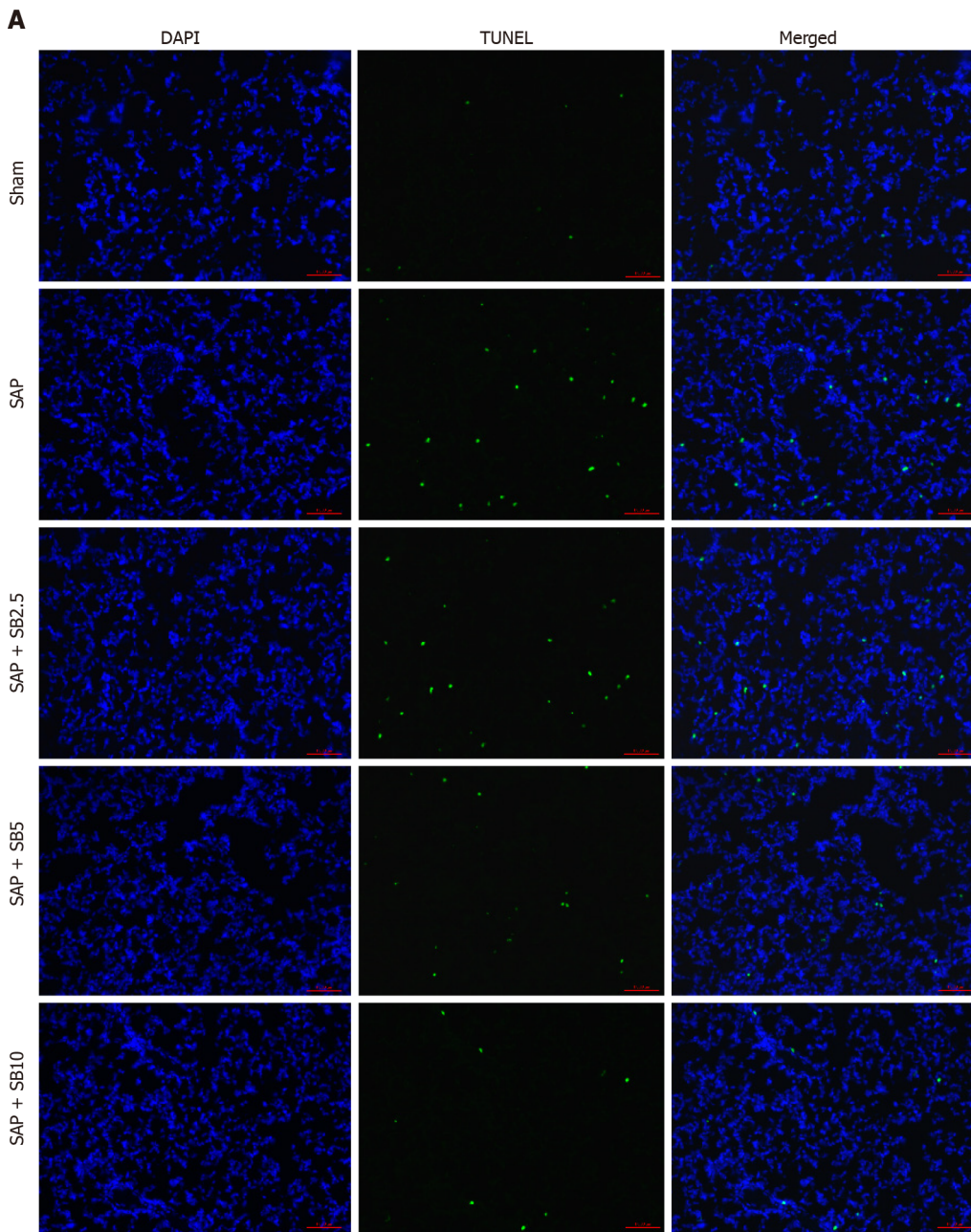


Figure 5 Effects of SB203580 on pulmonary capillary injury of severe acute pancreatitis rats. A: Evans blue extravasation in lung tissues; B: Bronchoalveolar protein concentration; C: Representative electron microscope photomicrographs of pulmonary microvascular endothelial cells in lung tissues; Sham group: Magnification 1500 × and 4000 ×, respectively; Severe acute pancreatitis (SAP) group: Magnification 1500 × and 5000 ×, respectively; SAP + SB10 group: Magnification 1500 × and 5000 ×, respectively; White arrows: Dense endothelial cell-cell junctions; White arrowheads: Low electron density clouds with an irregular thickness indicating basal membrane edema; Yellow arrows: Dissolution, rupture and debris of capillary endothelial; Orange star: Red blood cell. Data were expressed as mean ± SE; ^a*P* < 0.05 vs sham group; ^b*P* < 0.05 vs SAP group; ^c*P* < 0.05 vs SAP + SB2.5 group. SAP: Severe acute pancreatitis.

SB203580, no obvious rupture of endothelial cells or red cells extravasating from the vessels were observed.

SB203580 inhibits apoptosis in the lungs of SAP rats

TUNEL staining was used to examine cell death in lung tissues. Cell apoptosis in the lung tissues was assessed by the colocalization of TUNEL-green and DAPI-blue staining. A prominent increase in the number of positively stained cells was observed in the SAP group compared to the sham group, indicating a higher apoptotic rate (Figure 6A). Treatment of SAP rats with SB203580 significantly decreased the number of apoptotic cells, and the greatest inhibitory effect was observed in rats treated with 10.0 mg/kg SB203580. Proteins regulating the apoptotic signaling pathways were examined using western blotting to further confirm the cell death pathway. As shown in Figure 6B-E, although no change in the antiapoptotic protein Bcl2 was observed, the levels of the proapoptotic proteins Bax, Bim and cle-caspase3 were upregulated in the



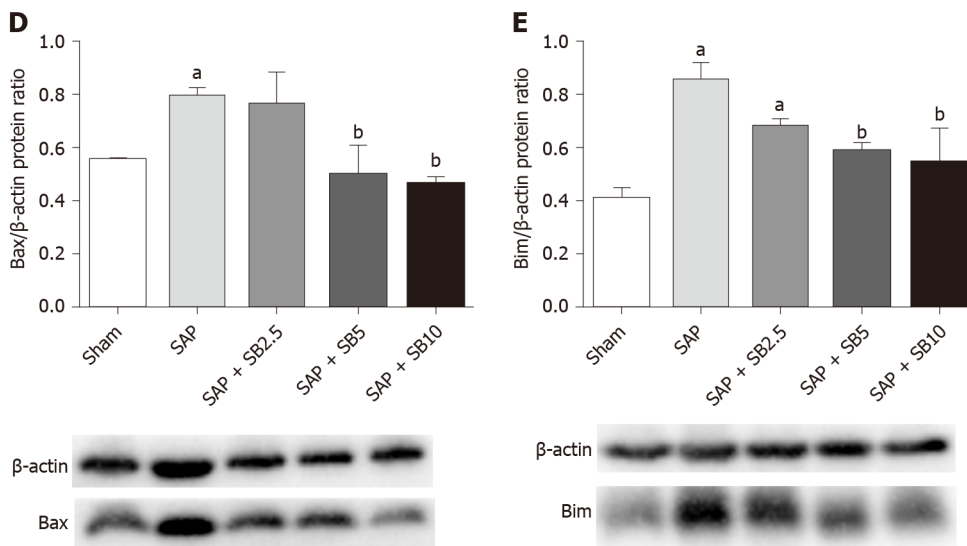


Figure 6 Effect of SB203580 on apoptosis of lung tissues in severe acute pancreatitis. A: Representative terminal deoxynucleotidyl transferase-mediated dUTP nick end labeling images of pulmonary sections (200 \times); B: Cle-caspase3; C: Bcl2; D: Bax; E: Bim. B-E: Representative western blotting analysis results for apoptosis-related proteins in lung tissues; Data were expressed as mean \pm SE; ^a $P < 0.05$ vs sham group; ^b $P < 0.05$ vs severe acute pancreatitis group. SAP: Severe acute pancreatitis.

SAP group compared to the sham group. SB203580 treatment reversed the changes in the levels of these proteins in the SAP group in a dose-dependent manner.

SB203580 protects against ALI by regulating proinflammatory and proapoptotic signaling pathways

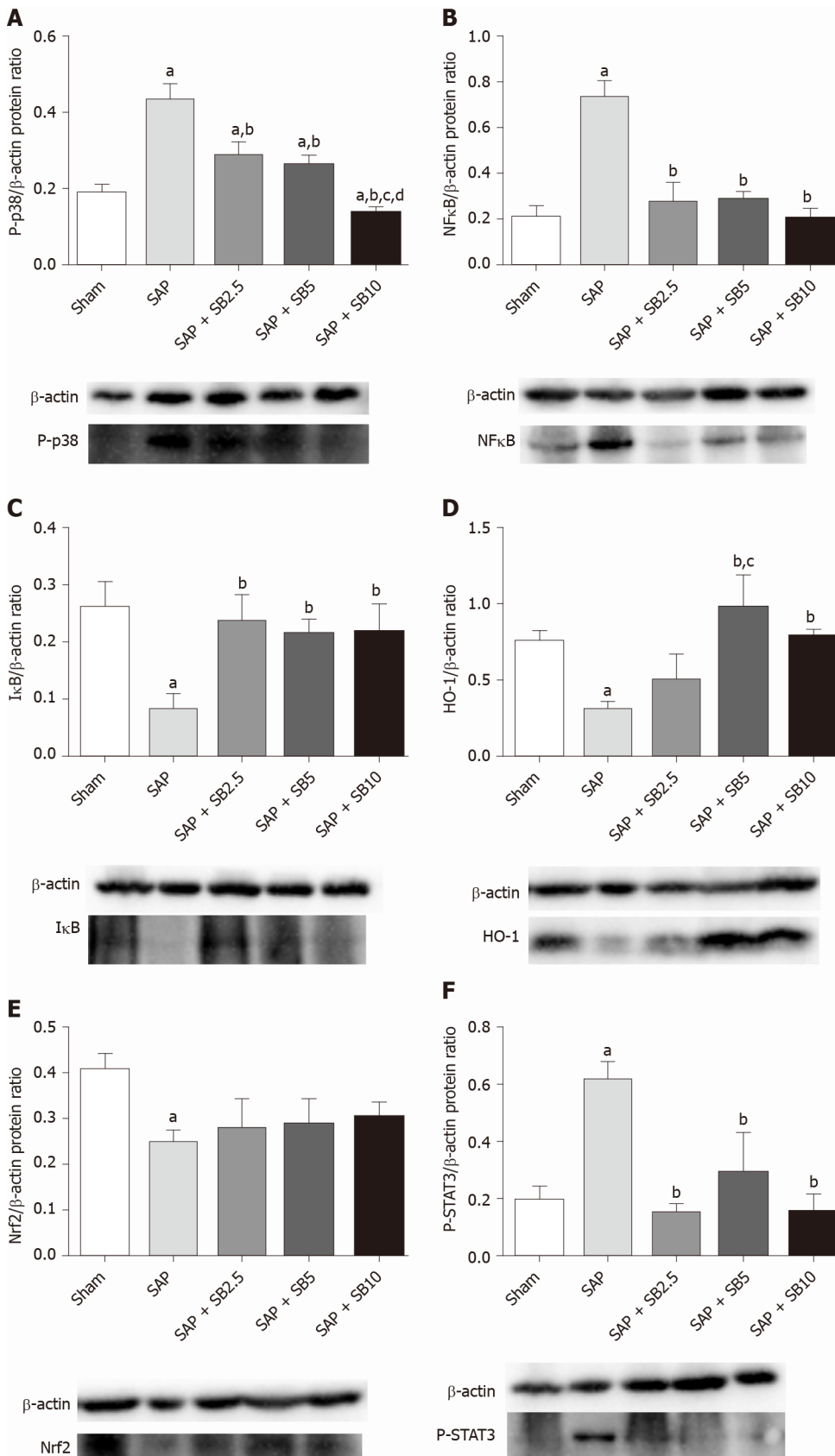
Levels of the P-p38, NF κ B, I κ B, Nrf2, HO-1, P-SATA3 and Myd88 proteins were detected in the lungs for further evaluation of the protective mechanism of SB203580. Figure 7 showed increased levels of P-p38, NF κ B, P-SATA3 and Myd88 but decreased levels of I κ B, Nrf2 and HO-1 in the SAP group compared with the sham group. Intriguingly, SB203580 reversed the changes in the levels of these proteins, reducing P-p38, NF κ B, P-SATA3 and Myd88 levels but increasing I κ B and HO-1 levels compared with the SAP group. However, except for P-p38 and HO-1, the improvement of these parameters was not positively related to the dose of SB203580. In addition, SB203580 slightly increased the level of Nrf2, but the difference was not statistically significant (Figure 7E).

DISCUSSION

Although the mechanisms of ALI/acute respiratory distress syndrome following SAP have not been completely elucidated, an increasing number of studies have described PMVEC injury and dysfunction as prerequisites for ALI[24]. The PMVECs are activated, participate in host defenses and result in increased microvascular permeability and damaged lung function[8,25]. Regardless of the etiology, an exaggerated inflammatory response is widely accepted to play a vital role in the transition of AP into a systemic disease[26]. Various inflammatory mediators have been related to AP severity and they induce their own or other mediators' secretion through a positive feedback mechanism, leading to amplification of the inflammatory cascade[27]. TNF- α was discovered to play a role in the early phase and cause the activation and injury of endothelial cells, functioning as a key promoter of the development of SAP-ALI[28]. In the present study, TNF- α was used to mimic SAP-related PMVEC injury *in vitro*.

p38 is activated by various insults, including cytokines, while the activation of p38 MAPK inevitably induces the expression of proinflammatory cytokines[29]. In our study, TNF- α induced higher levels of inflammatory cytokines (IL-1 β and IL-6) in PMVECs with p38 overactivation (Figure 1D and 1E). These results further confirmed a positive role for the p38 MAPK signaling pathway in regulating cytokine expression.

According to previous studies, p38 MAPK is involved in both survival and apoptosis pathways. It promotes anti- or proapoptotic effects in a cell type and



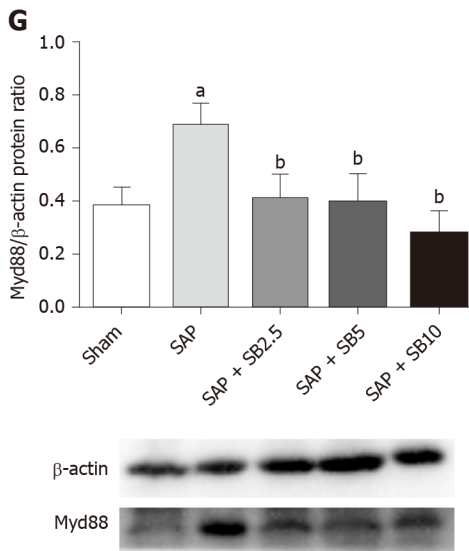


Figure 7 Effect of SB203580 on proinflammatory and proapoptotic signaling pathways. Representative Western blotting analysis results for protein expression in pulmonary tissue; A: P-p38; B: NFκB; C: IκB; D: HO-1; E: Nrf2; F: P-STAT3; G: Myd88. Data are expressed as mean ± SE; ^aP < 0.05 vs sham group; ^bP < 0.05 vs severe acute pancreatitis group; ^cP < 0.05 vs severe acute pancreatitis + SB2.5 group; ^dP < 0.05 vs severe acute pancreatitis + SB5 group. Nrf2: Nuclear factor erythroid 2-related factor 2; STAT3: Signal transducer and activator of transcription-3.

stimulus-specific manner in endothelial cells. For example, one group reported that SB203580 inhibited p38 MAPK and then decreased the endothelial cell apoptosis stimulated by TNF- α and cycloheximide[30], while another group illustrated that SB203580 enhanced endothelial cell apoptosis triggered by TNF- α alone[31]. It was reported that endothelial cells are relatively resistant to TNF- α , which induce only modest or no cell damage[31,32]. Then, we chose to overexpress activated MKK 6 (Glu) to constitutively activate p38 MAPK in PMVECs. Flow cytometry analysis revealed apoptotic cell death in null PMVECs stimulated with TNF- α , and MKK 6 (Glu) transfection resulted in a significantly higher apoptotic rate (Figure 1B). This finding indicated that persistent activation of p38 MAPK promotes TNF- α -induced PMVEC apoptosis. However, SB203580 pretreatment conversely aggravated PMVEC injury in this study (data not shown) and did not alleviate cell apoptosis. This discrepancy may be attributed to the extent or duration of p38 MAPK activation[33]. Rapid and transient p38 activation modulates inhibitors of the apoptosis protein family to prevent TNF- α -induced apoptosis[31], while sustained activation leads to apoptosis through the phosphorylation and downregulation of Bcl-x_i[30]. Therefore, SB203580 may exert a beneficial effect to maintain an appropriate level of p38 MAPK activity.

Many small-molecule inhibitors targeting p38 MAPK, such as SB203850, CNI-1493[34], SB202190[35], RWJ-67657[36] and UM101[37], have been tested in various cell injury or disease models. In AP, the p38 MAPK signaling pathway is involved not only in pancreatic acinar injury[20,38] but also in injury to distant organs (lung, liver, kidney, gut and placenta)[39-43]. SB203850 is a pyridinyl imidazole derivative that competes for ATP binding, and the inhibition of p38 MAPK has been shown to attenuate the severity of AP and its related distant organ injury[14,15,39,44]. In the present study, we treated SAP rats with SB203580 to investigate its protective effect on SAP-associated lung injury and the potential underlying mechanisms. As shown in Figure 2, SB203580 significantly alleviated pancreatic histopathological damage in SAP rats. Furthermore, it alleviated lung histopathological injuries (Figure 3), decreased the levels of inflammatory factors (IL-1 β , TNF- α , IL-6 and MPO, Figure 4) and preserved PaO₂, consistent with previous reports[14,15]. Based on these results, SB203580 effectively decreased the inflammatory response in rats with SAP-ALI. In addition, by analyzing three different doses of SB203580, we observed a dose-dependent improvement in the therapeutic effects, as 10.0 mg/kg was the most effective.

Although apoptosis is regarded as a protective mechanism, excessive apoptosis is harmful to the alveolar capillary membrane and pulmonary function. As the first-line responder to systemic injurious factor insults, damage to endothelial cells is detected earlier than damage to epithelial cells[45]. PMVEC damage results in lung injury, which in turn promotes the secretion of inflammatory mediators to destroy PMVECs in individuals with SAP[46]. In the present study, increased Evans blue extravasation

and BALF protein concentrations revealed increased capillary permeability in SAP rats. Moreover, transmission electron microscopy analysis directly confirmed capillary endothelial dissolution and rupture in the lung (Figure 5). Finally, the results of the TUNEL and western blot analyses (Figure 6) suggested that an increased number of apoptotic cells was involved in the pathological process of SAP-ALI. However, SB203580 significantly reversed the changes in Evans blue accumulation, BALF protein concentration, TUNEL-positive cells, apoptosis-regulated proteins and endothelial microstructure, providing evidence for the underlying protective effects of p38 MAPK inhibitors on endothelial cell apoptosis.

Because p38 MAPK is a proximal initiator of signal transduction, various substrates are directly or indirectly activated by p38 MAPK, permitting it to perform a wide range of functions[29,47]. The biological consequences of p38 MAPK inhibition are complicated by interactions with other signaling pathways. p38 MAPK was reported to have a dual function in regulating Nrf2/HO-1 signaling[48,49]. HO-1 possesses cytoprotective properties, including anti-inflammatory, antioxidant and antiapoptotic activities. NFκB, which is downstream of p38 MAPK, represses Nrf2 transcriptional activity[50,51], while HO-1 inhibits proinflammatory mediators through the inactivation of NFκB[52]. STAT3 is activated by p38 MAPK, transferring signals to the nucleus and regulating gene expression[53,54]. MyD88 is considered a classical proinflammatory and proapoptotic upstream signaling adaptor molecule of p38 MAPK[55]. While the mechanism underlying the effects of SB203580 must be further elucidated, the levels of these key proteins involved in inflammatory, oxidative and apoptotic signaling pathways were measured. In the present study, SB203580 treatment reversed the increased levels of P-p38, NFκB, P-STAT3 and Myd88 and decreased levels of IκB and HO-1 in the SAP group (Figure 7). Therefore, the protective effects of p38 inhibition *via* SB203580 were likely partially attributed to the inhibition of pulmonary proinflammatory and proapoptotic signaling pathways.

CONCLUSION

In conclusion, p38 MAPK overactivation promoted TNF-α-induced inflammatory cytokine expression and PMVEC apoptosis *in vitro*. The inhibition of p38 MAPK with SB203580 protected against SAP-ALI by alleviating inflammation and apoptotic cell death in rats. Therefore, SB203580 may alleviate SAP-ALI by inhibiting the proinflammatory and proapoptotic effects of the p38 MAPK pathway on PMVECs. These results suggest the possibility of applying p38 MAPK inhibitors as treatments for SAP-ALI in the clinical setting.

ARTICLE HIGHLIGHTS

Research background

Acute lung injury (ALI) is the main reason for the high mortality of patients with severe acute pancreatitis (SAP). Injury and dysfunction of pulmonary microvascular endothelial cells (PMVEC) are considered prerequisites for ALI. The p38 mitogen-activated protein kinase (p38 MAPK) signaling pathway is involved in the development of SAP-related ALI. However, the precise mechanism by which p38 MAPK regulates PMVEC injury in SAP-related ALI is unclear.

Research motivation

To date, no specific pharmacological therapies for SAP associated ALI are available. Elucidating the mechanism of PMVEC injury regulated by p38 MAPK is expected to help identify new treatments for SAP-associated ALI.

Research objectives

To determine the role of p38 MAPK in the tumor necrosis factor-α-induced injury of PMVECs *in vitro* and to explore the effect of SB203580-mediated p38 inhibition on SAP-ALI *in vivo*.

Research methods

In vitro, PMVECs were transfected with MAPK kinase 6 (Glu) and stimulated with tumor necrosis factor-α to detect cell apoptosis and inflammatory cytokine levels.

In vivo, SAP-ALI rats were treated with three different doses of SB203580 (2.5, 5.0 or 10.0 mg/kg). Blood, bronchoalveolar lavage fluid and tissue samples were harvested to assess cytokine levels, blood gas analyses, histopathological changes, myeloperoxidase activity, bronchoalveolar protein concentration, Evans blue extravasation, apoptosis and ultrastructural changes of PMVECs. Then, the mechanism underlying the effects of SB203580 was also detected in the lungs.

Research results

In vitro, MAPK kinase (Glu) transfection resulted in higher apoptotic rates and cytokine levels in TNF- α -treated PMVECs. *In vivo*, SB203580 attenuated lung histopathological injury, decreased inflammatory activity and preserved pulmonary function. Furthermore, SB203580 significantly reversed the microvascular permeability, the increase in the number of terminal deoxynucleotidyl transferase-mediated dUTP nick end labeling-positive cells, the increased expression of apoptosis-related proteins and the endothelial microstructure changes. Moreover, SB203580 significantly reduced pulmonary P-p38, NF κ B, P-SATA3 and Myd88 levels but increased the I κ B and HO-1 levels.

Research conclusions

p38 inhibition may protect against SAP-ALI by alleviating inflammation and the apoptotic death of PMVECs.

Research perspectives

In this study, p38 MAPK overactivation promoted PMVEC injury *in vitro*, while p38 inhibition protected against SAP-ALI *in vivo*. These results suggest the potential of applying p38 MAPK inhibitors as treatments for SAP-ALI in the clinical setting.

REFERENCES

- 1 Forsmark CE, Vege SS, Wilcox CM. Acute Pancreatitis. *N Engl J Med* 2016; **375**: 1972-1981 [PMID: 27959604 DOI: 10.1056/NEJMra1505202]
- 2 Banks PA, Bollen TL, Dervenis C, Gooszen HG, Johnson CD, Sarr MG, Tsiotos GG, Vege SS; Acute Pancreatitis Classification Working Group. Classification of acute pancreatitis--2012: revision of the Atlanta classification and definitions by international consensus. *Gut* 2013; **62**: 102-111 [PMID: 23100216 DOI: 10.1136/gutjnl-2012-302779]
- 3 Elder AS, Saccone GT, Dixon DL. Lung injury in acute pancreatitis: mechanisms underlying augmented secondary injury. *Pancreatology* 2012; **12**: 49-56 [PMID: 22487475 DOI: 10.1016/j.pan.2011.12.012]
- 4 De Campos T, Deree J, Coimbra R. From acute pancreatitis to end-organ injury: mechanisms of acute lung injury. *Surg Infect (Larchmt)* 2007; **8**: 107-120 [PMID: 17381402 DOI: 10.1089/sur.2006.011]
- 5 Matthay MA, Zemans RL. The acute respiratory distress syndrome: pathogenesis and treatment. *Annu Rev Pathol* 2011; **6**: 147-163 [PMID: 20936936 DOI: 10.1146/annurev-pathol-011110-130158]
- 6 Aldridge AJ. Role of the neutrophil in septic shock and the adult respiratory distress syndrome. *Eur J Surg* 2002; **168**: 204-214 [PMID: 12440757 DOI: 10.1080/11024150260102807]
- 7 Fang M, Zhong WH, Song WL, Deng YY, Yang DM, Xiong B, Zeng HK, Wang HD. Ulinastatin Ameliorates Pulmonary Capillary Endothelial Permeability Induced by Sepsis Through Protection of Tight Junctions via Inhibition of TNF- α and Related Pathways. *Front Pharmacol* 2018; **9**: 823 [PMID: 30150933 DOI: 10.3389/fphar.2018.00823]
- 8 Maniatis NA, Kotanidou A, Catravas JD, Orfanos SE. Endothelial pathomechanisms in acute lung injury. *Vascul Pharmacol* 2008; **49**: 119-133 [PMID: 18722553 DOI: 10.1016/j.vph.2008.06.009]
- 9 Lum H, Malik AB. Mechanisms of increased endothelial permeability. *Can J Physiol Pharmacol* 1996; **74**: 787-800 [PMID: 8946065 DOI: 10.1139/y96-081]
- 10 Suzuki T, Sakata K, Mizuno N, Palikhe S, Yamashita S, Hattori K, Matsuda N, Hattori Y. Different involvement of the MAPK family in inflammatory regulation in human pulmonary microvascular endothelial cells stimulated with LPS and IFN- γ . *Immunobiology* 2018; **223**: 777-785 [PMID: 30115376 DOI: 10.1016/j.imbio.2018.08.003]
- 11 Maniatis NA, Orfanos SE. The endothelium in acute lung injury/acute respiratory distress syndrome. *Curr Opin Crit Care* 2008; **14**: 22-30 [PMID: 18195622 DOI: 10.1097/MCC.0b013e3282f269b9]
- 12 Yang Y, Li Q, Deng Z, Zhang Z, Xu J, Qian G, Wang G. Protection from lipopolysaccharide-induced pulmonary microvascular endothelial cell injury by activation of hedgehog signaling pathway. *Mol Biol Rep* 2011; **38**: 3615-3622 [PMID: 21110116 DOI: 10.1007/s11033-010-0473-8]
- 13 de Campos T, Deree J, Martins JO, Loomis WH, Shenvi E, Putnam JG, Coimbra R. Pentoxifylline attenuates pulmonary inflammation and neutrophil activation in experimental acute pancreatitis. *Pancreas* 2008; **37**: 42-49 [PMID: 18580443 DOI: 10.1097/MPA.0b013e3181612d19]

- 14 **Zhou Y**, Xia H, Zhao L, Mei F, Li M, You Y, Zhao K, Wang W. SB203580 attenuates acute lung injury and inflammation in rats with acute pancreatitis in pregnancy. *Inflammopharmacology* 2019; **27**: 99-107 [PMID: 30094758 DOI: 10.1007/s10787-018-0522-9]
- 15 **Cao MH**, Xu J, Cai HD, Lv ZW, Feng YJ, Li K, Chen CQ, Li YY. p38 MAPK inhibition alleviates experimental acute pancreatitis in mice. *Hepatobiliary Pancreat Dis Int* 2015; **14**: 101-106 [PMID: 25655298 DOI: 10.1016/s1499-3872(15)60327-7]
- 16 **Yang J**, Denham W, Tracey KJ, Wang H, Kramer AA, Salhab KF, Norman J. The physiologic consequences of macrophage pacification during severe acute pancreatitis. *Shock* 1998; **10**: 169-175 [PMID: 9744644 DOI: 10.1097/00024382-199809000-00004]
- 17 **King J**, Hamil T, Creighton J, Wu S, Bhat P, McDonald F, Stevens T. Structural and functional characteristics of lung macro- and microvascular endothelial cell phenotypes. *Microvasc Res* 2004; **67**: 139-151 [PMID: 15020205 DOI: 10.1016/j.mvr.2003.11.006]
- 18 **Li L**, Hu J, He T, Zhang Q, Yang X, Lan X, Zhang D, Mei H, Chen B, Huang Y. P38/MAPK contributes to endothelial barrier dysfunction via MAP4 phosphorylation-dependent microtubule disassembly in inflammation-induced acute lung injury. *Sci Rep* 2015; **5**: 8895 [PMID: 25746230 DOI: 10.1038/srep08895]
- 19 **Hu JY**, Chu ZG, Han J, Dang YM, Yan H, Zhang Q, Liang GP, Huang YS. The p38/MAPK pathway regulates microtubule polymerization through phosphorylation of MAP4 and Op18 in hypoxic cells. *Cell Mol Life Sci* 2010; **67**: 321-333 [PMID: 19915797 DOI: 10.1007/s00018-009-0187-z]
- 20 **Ren HB**, Li ZS, Xu GM, Tu ZX, Shi XG, Jia YT, Gong YF. Dynamic changes of mitogen-activated protein kinase signal transduction in rats with severe acute pancreatitis. *Chin J Dig Dis* 2004; **5**: 123-125 [PMID: 15612248 DOI: 10.1111/j.1443-9573.2004.00162.x]
- 21 **Zemans RL**, Colgan SP, Downey GP. Transepithelial migration of neutrophils: mechanisms and implications for acute lung injury. *Am J Respir Cell Mol Biol* 2009; **40**: 519-535 [PMID: 18978300 DOI: 10.1165/rcmb.2008-0348TR]
- 22 **Schmidt J**, Rattner DW, Lewandrowski K, Compton CC, Mandavilli U, Knoefel WT, Warshaw AL. A better model of acute pancreatitis for evaluating therapy. *Ann Surg* 1992; **215**: 44-56 [PMID: 1731649 DOI: 10.1097/00000658-199201000-00007]
- 23 **Dawra R**, Ku YS, Sharif R, Dhaukhandi D, Phillips P, Dudeja V, Saluja AK. An improved method for extracting myeloperoxidase and determining its activity in the pancreas and lungs during pancreatitis. *Pancreas* 2008; **37**: 62-68 [PMID: 18580446 DOI: 10.1097/MPA.0b013e3181607761]
- 24 **Ye W**, Zheng C, Yu D, Zhang F, Pan R, Ni X, Shi Z, Zhang Z, Xiang Y, Sun H, Shi K, Chen B, Zhang Q, Zhou M. Lipoxin A4 Ameliorates Acute Pancreatitis-Associated Acute Lung Injury through the Antioxidative and Anti-Inflammatory Effects of the Nrf2 Pathway. *Oxid Med Cell Longev* 2019; **2019**: 2197017 [PMID: 31781326 DOI: 10.1155/2019/2197017]
- 25 **Yi L**, Huang X, Guo F, Zhou Z, Chang M, Huan J. GSK-3 β -Dependent Activation of GEF-H1/ROCK Signaling Promotes LPS-Induced Lung Vascular Endothelial Barrier Dysfunction and Acute Lung Injury. *Front Cell Infect Microbiol* 2017; **7**: 357 [PMID: 28824887 DOI: 10.3389/fcimb.2017.00357]
- 26 **Yang X**, Zhang X, Lin Z, Guo J, Yang X, Yao L, Wang H, Xue P, Xia Q. Chaiqin chengqi decoction alleviates severe acute pancreatitis associated acute kidney injury by inhibiting endoplasmic reticulum stress and subsequent apoptosis. *Biomed Pharmacother* 2020; **125**: 110024 [PMID: 32187959 DOI: 10.1016/j.biopha.2020.110024]
- 27 **Sandoval J**, Pereda J, Pérez S, Finamor I, Vallet-Sánchez A, Rodríguez JL, Franco L, Sastre J, López-Rodas G. Epigenetic Regulation of Early- and Late-Response Genes in Acute Pancreatitis. *J Immunol* 2016; **197**: 4137-4150 [PMID: 27798150 DOI: 10.4049/jimmunol.1502378]
- 28 **Yu S**, Xie J, Xiang Y, Dai S, Yu D, Sun H, Chen B, Zhou M. Downregulation of TNF- α /TNF-R1 Signals by AT-Lipoxin A4 May Be a Significant Mechanism of Attenuation in SAP-Associated Lung Injury. *Mediators Inflamm* 2019; **2019**: 9019404 [PMID: 31097921 DOI: 10.1155/2019/9019404]
- 29 **Viemann D**, Goebeler M, Schmid S, Klimmek K, Sorg C, Ludwig S, Roth J. Transcriptional profiling of IKK2/NF-kappa B- and p38 MAP kinase-dependent gene expression in TNF-alpha-stimulated primary human endothelial cells. *Blood* 2004; **103**: 3365-3373 [PMID: 14715628 DOI: 10.1182/blood-2003-09-3296]
- 30 **Grethe S**, Ares MP, Andersson T, Pörn-Ares MI. p38 MAPK mediates TNF-induced apoptosis in endothelial cells via phosphorylation and downregulation of Bcl-x(L). *Exp Cell Res* 2004; **298**: 632-642 [PMID: 15265709 DOI: 10.1016/j.yexcr.2004.05.007]
- 31 **Furusu A**, Nakayama K, Xu Q, Konta T, Kitamura M. MAP kinase-dependent, NF-kappaB-independent regulation of inhibitor of apoptosis protein genes by TNF-alpha. *J Cell Physiol* 2007; **210**: 703-710 [PMID: 17133355 DOI: 10.1002/jcp.20881]
- 32 **Roulston A**, Reinhard C, Amiri P, Williams LT. Early activation of c-Jun N-terminal kinase and p38 kinase regulate cell survival in response to tumor necrosis factor alpha. *J Biol Chem* 1998; **273**: 10232-10239 [PMID: 9553074 DOI: 10.1074/jbc.273.17.10232]
- 33 **Matsuzawa A**, Ichijo H. Stress-responsive protein kinases in redox-regulated apoptosis signaling. *Antioxid Redox Signal* 2005; **7**: 472-481 [PMID: 15706095 DOI: 10.1089/ars.2005.7.472]
- 34 **Yang J**, Murphy C, Denham W, Botchkina G, Tracey KJ, Norman J. Evidence of a central role for p38 map kinase induction of tumor necrosis factor alpha in pancreatitis-associated pulmonary injury. *Surgery* 1999; **126**: 216-222 [PMID: 10455887]
- 35 **Lüschen S**, Scherer G, Ussat S, Ungefroren H, Adam-Klages S. Inhibition of p38 mitogen-activated protein kinase reduces TNF-induced activation of NF-kappaB, elicits caspase activity, and enhances

- cytotoxicity. *Exp Cell Res* 2004; **293**: 196-206 [PMID: 14729457 DOI: 10.1016/j.yexcr.2003.10.009]
- 36 **Kuldo JM**, Westra J, Asgeirsdóttir SA, Kok RJ, Oosterhuis K, Rots MG, Schouten JP, Limburg PC, Molema G. Differential effects of NF- κ B and p38 MAPK inhibitors and combinations thereof on TNF- α - and IL-1 β -induced proinflammatory status of endothelial cells in vitro. *Am J Physiol Cell Physiol* 2005; **289**: C1229-C1239 [PMID: 15972838 DOI: 10.1152/ajpcell.00620.2004]
- 37 **Shah NG**, Tulapurkar ME, Ramarathnam A, Brophy A, Martinez R 3rd, Hom K, Hodges T, Samadani R, Singh IS, MacKerell AD Jr, Shapiro P, Hasday JD. Novel Noncatalytic Substrate-Selective p38 α -Specific MAPK Inhibitors with Endothelial-Stabilizing and Anti-Inflammatory Activity. *J Immunol* 2017; **198**: 3296-3306 [PMID: 28298524 DOI: 10.4049/jimmunol.1602059]
- 38 **Twait E**, Williard DE, Samuel I. Dominant negative p38 mitogen-activated protein kinase expression inhibits NF- κ B activation in AR42J cells. *Pancreatol* 2010; **10**: 119-128 [PMID: 20453549 DOI: 10.1159/000290656]
- 39 **Ouyang J**, Zhang ZH, Zhou YX, Niu WC, Zhou F, Shen CB, Chen RG, Li X. Up-regulation of Tight-Junction Proteins by p38 Mitogen-Activated Protein Kinase/p53 Inhibition Leads to a Reduction of Injury to the Intestinal Mucosal Barrier in Severe Acute Pancreatitis. *Pancreas* 2016; **45**: 1136-1144 [PMID: 27171513 DOI: 10.1097/MPA.0000000000000656]
- 40 **Fan HN**, Chen W, Fan LN, Wu JT, Zhu JS, Zhang J. Macrophages-derived p38 α promotes the experimental severe acute pancreatitis by regulating inflammation and autophagy. *Int Immunopharmacol* 2019; **77**: 105940 [PMID: 31655340 DOI: 10.1016/j.intimp.2019.105940]
- 41 **Wang B**, Zhao KL, Hu WJ, Zuo T, Ding YM, Wang WX. Macrophage Migration Inhibitor Promoted the Intrahepatic Bile Duct Injury in Rats with Severe Acute Pancreatitis. *Dig Dis Sci* 2019; **64**: 759-772 [PMID: 30465176 DOI: 10.1007/s10620-018-5379-7]
- 42 **Li M**, Yu J, Zhao L, Mei FC, Zhou Y, Hong YP, Zuo T, Wang WX. Inhibition of macrophage migration inhibitory factor attenuates inflammation and fetal kidney injury in a rat model of acute pancreatitis in pregnancy. *Int Immunopharmacol* 2019; **68**: 106-114 [PMID: 30622028 DOI: 10.1016/j.intimp.2018.12.068]
- 43 **Zuo T**, Yu J, Wang WX, Zhao KL, Chen C, Deng WH, He XB, Wang P, Shi Q, Guo WY. Mitogen-Activated Protein Kinases Are Activated in Placental Injury in Rat Model of Acute Pancreatitis in Pregnancy. *Pancreas* 2016; **45**: 850-857 [PMID: 26491907 DOI: 10.1097/MPA.0000000000000528]
- 44 **Wan YD**, Zhu RX, Bian ZZ, Pan XT. Improvement of Gut Microbiota by Inhibition of P38 Mitogen-Activated Protein Kinase (MAPK) Signaling Pathway in Rats with Severe Acute Pancreatitis. *Med Sci Monit* 2019; **25**: 4609-4616 [PMID: 31226101 DOI: 10.12659/MSM.914538]
- 45 **Wang F**, Lu F, Huang H, Huang M, Luo T. Ultrastructural changes in the pulmonary mechanical barriers in a rat model of severe acute pancreatitis-associated acute lung injury. *Ultrastruct Pathol* 2016; **40**: 33-42 [PMID: 26512751 DOI: 10.3109/01913123.2015.1088907]
- 46 **Han X**, Wang Y, Chen H, Zhang J, Xu C, Li J, Li M. Enhancement of ICAM-1 via the JAK2/STAT3 signaling pathway in a rat model of severe acute pancreatitis-associated lung injury. *Exp Ther Med* 2016; **11**: 788-796 [PMID: 26997994 DOI: 10.3892/etm.2016.2988]
- 47 **Hoefen RJ**, Berk BC. The role of MAP kinases in endothelial activation. *Vascul Pharmacol* 2002; **38**: 271-273 [PMID: 12487031 DOI: 10.1016/s1537-1891(02)00251-3]
- 48 **Naidu S**, Vijayan V, Santoso S, Kietzmann T, Immenschuh T. Inhibition and genetic deficiency of p38 MAPK up-regulates heme oxygenase-1 gene expression via Nrf2. *J Immunol* 2009; **182**: 7048-7057 [PMID: 19454702 DOI: 10.4049/jimmunol.0900006]
- 49 **Zhou MM**, Zhang WY, Li RJ, Guo C, Wei SS, Tian XM, Luo J, Kong LY. Anti-inflammatory activity of Khayandirobilide A from *Khaya senegalensis* via NF- κ B, AP-1 and p38 MAPK/Nrf2/HO-1 signaling pathways in lipopolysaccharide-stimulated RAW 264.7 and BV-2 cells. *Phytomedicine* 2018; **42**: 152-163 [PMID: 29655681 DOI: 10.1016/j.phymed.2018.03.016]
- 50 **Reboll MR**, Schweda AT, Bartels M, Franke R, Frank R, Nourbakhsh M. Mapping of NRF binding motifs of NF- κ B p65 subunit. *J Biochem* 2011; **150**: 553-562 [PMID: 21821668 DOI: 10.1093/jb/mvr099]
- 51 **Niedick I**, Froese N, Oumard A, Mueller PP, Nourbakhsh M, Hauser H, Köster M. Nucleolar localization and mobility analysis of the NF- κ B repressing factor NRF. *J Cell Sci* 2004; **117**: 3447-3458 [PMID: 15226370 DOI: 10.1242/jcs.01129]
- 52 **Ha YM**, Kim MY, Park MK, Lee YS, Kim YM, Kim HJ, Lee JH, Chang KC. Higenamine reduces HMGB1 during hypoxia-induced brain injury by induction of heme oxygenase-1 through PI3K/Akt/Nrf-2 signal pathways. *Apoptosis* 2012; **17**: 463-474 [PMID: 22183510 DOI: 10.1007/s10495-011-0688-8]
- 53 **Stephanou A**, Latchman DS. Opposing actions of STAT-1 and STAT-3. *Growth Factors* 2005; **23**: 177-182 [PMID: 16243709 DOI: 10.1080/08977190500178745]
- 54 **Ng DC**, Long CS, Bogoyevitch MA. A role for the extracellular signal-regulated kinase and p38 mitogen-activated protein kinases in interleukin-1 β -stimulated delayed signal transducer and activator of transcription 3 activation, atrial natriuretic factor expression, and cardiac myocyte morphology. *J Biol Chem* 2001; **276**: 29490-29498 [PMID: 11382751 DOI: 10.1074/jbc.M100699200]
- 55 **Shih JH**, Tsai YF, Li IH, Chen MH, Huang YS. Hp-s1 Ganglioside Suppresses Proinflammatory Responses by Inhibiting MyD88-Dependent NF- κ B and JNK/p38 MAPK Pathways in Lipopolysaccharide-Stimulated Microglial Cells. *Mar Drugs* 2020; **18** [PMID: 33003399 DOI: 10.3390/md18100496]



Published by **Baishideng Publishing Group Inc**
7041 Koll Center Parkway, Suite 160, Pleasanton, CA 94566, USA
Telephone: +1-925-3991568
E-mail: bpgoffice@wjgnet.com
Help Desk: <https://www.f6publishing.com/helpdesk>
<https://www.wjgnet.com>

